



# A Two-point Method for Multiaxial Fatigue Life Prediction

Jianhui Liu<sup>1</sup>   Xuemei Pan<sup>1\*</sup>    Youtang Li<sup>1</sup>   Xiaochuang Chen<sup>2</sup>

<sup>(1)</sup>*School of Mechanical and Electrical Engineering, Lanzhou University of Technology, Lanzhou 730050, China*

<sup>(2)</sup>*Lanzhou Jinchuan Advanced Materials Technology Co., Ltd., Lanzhou 730101, China*

Received 9 June 2021; revision received 29 September 2021; Accepted 7 October 2021;  
published online 12 January 2022

© The Chinese Society of Theoretical and Applied Mechanics 2022

**ABSTRACT** Fatigue fracture is one of the most common failure modes of engineering components, and the combined action of geometric discontinuity and multiaxial loading is more likely to cause severe fatigue damage of components. This work focuses on the fatigue behavior of U-notched Q345 steel specimens with different notch sizes under proportional cyclic tension–torsion. Firstly, based on the concept of strain energy, the calculation method of critical plane is given and the equivalent stress of the specified path on the critical plane is extracted to characterize the equivalent stress distribution state and the stress gradient effect. Then, based on the high stress volume method and theory of critical distance, a simple method for determining the critical distance is given considering the contribution of stress at the dangerous point and the critical point. In addition, based on the idea of stress–distance normalization, a new stress gradient impact factor is defined and a new method for predicting the multiaxial fatigue life of notched specimens is given. The prediction results of the proposed model, the local stress–strain method and the point method of theory of critical distance are compared with the experimental results. The comparisons show that the prediction results of the proposed model are closer to experimental life, and the calculation accuracy is higher.

**KEY WORDS** Multiaxial fatigue, Stress gradient, Life prediction, Critical distance method, Local stress–strain method

## 1. Introduction

In mechanical engineering, there are many components with sudden changes in size due to various functional requirements, such as pressure vessels and mining machinery [1], and these structures are normally called notched components during fatigue failure analysis. As we all know, the notch effect exists at notch root inevitably, and local plastic deformation occurs when the stress at the root of notch reaches the yield limit. So the internal low-stress region still supports the high-stress region of the notch, which retards the initiation and propagation of fatigue cracks and delays the fatigue failure process of the structure. Meanwhile, these components are mostly subjected to complex cyclic loading; even in the uniaxial loading, the notch area is in a complex multiaxial stress field, especially under the multiaxial loading [2]. During the entire service period, due to the combined effect of notch and stress multi-axiality at the notch root, fatigue damage near the notch gradually accumulates and becomes more severe relative to the non-notched area, which leads to the deterioration of local mechanical

\* Corresponding author. E-mail: panxuemeilut@163.com

performance until fatigue fracture failure occurs. Thus, it is significant to study the fatigue properties of notched parts under complex multiaxial cyclic loading in engineering applications.

Over the past few decades, several methods such as the nominal stress method [3], the local stress-strain method [4], the stress field intensity method [5], and the critical distance method [6] have been developed in response to the fatigue problems of notched parts. Among them, the local stress-strain method takes the maximum stress and strain at the tip of the notch as damage parameters to carry out fatigue analysis [4]. Due to its simple calculation process, this method is still widely used in engineering. Recent studies [7] show that the calculation results of the local stress-strain method are relatively accurate when the stress gradient in the local region of the notch is low. However, if there is an obvious stress gradient at the root of the notch, this method will cause larger calculation errors, and the calculation results tend to be more conservative. This is because the local stress-strain method only considers the local stress and strain state at the root of the notch, and the stress gradient caused by the notch effect is ignored.

Taylor et al. [8] presented the theory of critical distance (TCD) based on the ideas of Neuber [9] and Peterson [10]. They believed that the linear-elastic stress distribution state within a certain area in the vicinity of the notch root would have an impact on the fatigue characteristics of the specimens. Later, different scholars took the stresses averaged in the vicinity of the notch root as the fatigue damage parameter, and developed some different notch fatigue analysis approaches. Initially, Neuber [9] proposed the line method (LM) to average the stress within a certain critical distance from the root of the notch. Then, Peterson [10] presented the point method (PM) and took the stress at the specified point as the fatigue damage parameter to predict the life of the specimens. Later, Taylor [11] and Bellett et al. [12] developed the area method and the volume method, respectively. Among these four methods, the PM and LM were widely used because of their simple calculation processes. The expressions for these four methods are given as follows:

$$\text{the point method (PM): } \sigma_{\text{av}} = \sigma_1 \left( r = \frac{L_0}{2}, \theta = 0 \right) \quad (1)$$

$$\text{the line method (LM): } \sigma_{\text{av}} = \frac{1}{2L_0} \int_0^{2L_0} \sigma_1(r, \theta = 0) dr \quad (2)$$

$$\text{the area method (AM): } \sigma_{\text{av}} = \frac{2}{1.1\pi L_0^2} \int_{-\pi/2}^{\pi/2} \int_0^{L_0} \sigma_1(r, \theta) r dr d\theta \quad (3)$$

$$\text{the volume method (VM): } \sigma_{\text{av}} = \frac{3}{2\pi(1.54L_0)^3} \int_0^{2\pi} \int_0^{\pi/2} \int_0^{1.54L_0} \sigma_1(r, \theta, \varphi) r^2 \sin \theta dr d\theta d\varphi \quad (4)$$

where  $\sigma_{\text{av}}$  is the average stress within the critical distance,  $\sigma_1$  is the maximum principal stress at polar coordinates  $(r, \theta, \varphi)$ , and  $L_0$  is the critical distance.

TCD has been widely used because it considers the influence of stress/strain gradient on crack initiation, which weakens the effect of the maximum stress at the dangerous point. So, the prediction results of TCD are closer to real fatigue life and the calculation accuracy is relatively high [7]. This approach has attracted extensive attention from many scholars. Combining with the PM of TCD, Susmel [13] took the plane with maximum shear stress as the critical plane and used the modified Wöhler curve method to calculate fatigue life. Wu [14] proposed a fatigue life calculation method based on the PM and the LM to modify the root damage gradient of the notch under multiaxial loading. However, when TCD is used to determine the effective stress, it is difficult to determine the critical distance  $L_0$ .

In this paper, a multiaxial fatigue life prediction model for notched specimens considering equivalent stress gradient effect and size effect under multiaxial proportional loading is presented based on the high stress volume method and the critical plane theory. Firstly, based on the concept of strain energy, the calculation method of critical plane is given and the equivalent stress of the specified path on the critical plane is extracted to characterize the equivalent stress distribution state. Then, the position

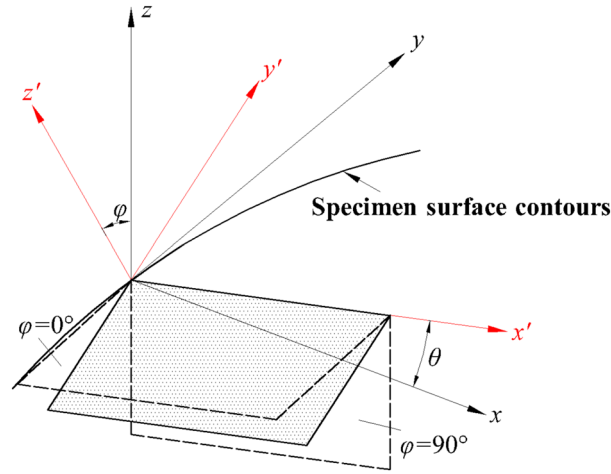


Fig. 1. Coordinate transformation diagram

of 95% of peak equivalent stress is determined, called the critical point; and the distance between the dangerous point and the critical point is defined as the critical distance. In order to consider the combined effect of peak equivalent stress and the equivalent stress at the critical point, the two-point method is proposed to calculate the effective stress based on the PM of TCD. In addition, the impact factor of equivalent stress gradient is defined to characterize the influence of equivalent stress gradient at the notch, and a new model is finally established to predict the fatigue life of notched Q345 steel specimens. The feasibility of the model is verified by comparing the prediction results with the experimental results and those of the local stress-strain method and the PM of TCD.

## 2. Determination of the Critical Plane and Critical Distance

Firstly, elastic-plastic finite-element software is used to analyze the mechanical properties of the specimens. According to the hardening laws of the materials, the Bauschinger effect of the materials is described by the multilinear kinematic hardening (MKIN) model, and the cyclic loading is realized by setting load steps in finite element software. So the stress and strain history of the notch root in a single cycle is obtained. Then, the location of the dangerous point of the specimens is determined, and the stress-strain state of the dangerous point in the basic coordinate system  $xyz$  can be extracted. With the help of the coordinate transformation matrix, the stress-strain states of an arbitrary material plane passing through the dangerous point are obtained. Finally, based on the energy method, the strain energy function  $f(\theta, \varphi)$  of an arbitrary material plane can be established. Meanwhile, the stagnation point of the strain energy function can be calculated by taking the partial derivative of  $\theta$  and  $\varphi$ , respectively, and the position of the critical plane can be finally determined.

### 2.1. Coordinate Transformation Principle

In order to get the stress and strain components on an arbitrary material plane through the dangerous point, the coordinate transformation method is used. Firstly, a new coordinate plane  $x' - y'$  can be obtained by rotating the  $x - y$  plane around the  $z$ -axis and with a rotation angle of  $\theta$ . Then, a new coordinate axis  $z'$  can be obtained by rotating the  $z$ -axis around the  $x'$ -axis and with a rotation angle of  $\varphi$ . The diagram is shown in Fig. 1.

The stress tensor  $\sigma_{ij}$  and strain tensor  $\varepsilon_{ij}$  in the basic coordinate system  $xyz$  are given as follows:

$$\sigma_{ij} = \begin{bmatrix} \sigma_{11} & \sigma_{12} & \sigma_{13} \\ \sigma_{21} & \sigma_{22} & \sigma_{23} \\ \sigma_{31} & \sigma_{32} & \sigma_{33} \end{bmatrix}; \quad \varepsilon_{ij} = \begin{bmatrix} \varepsilon_{11} & \varepsilon_{12} & \varepsilon_{13} \\ \varepsilon_{21} & \varepsilon_{22} & \varepsilon_{23} \\ \varepsilon_{31} & \varepsilon_{32} & \varepsilon_{33} \end{bmatrix} \quad (5)$$

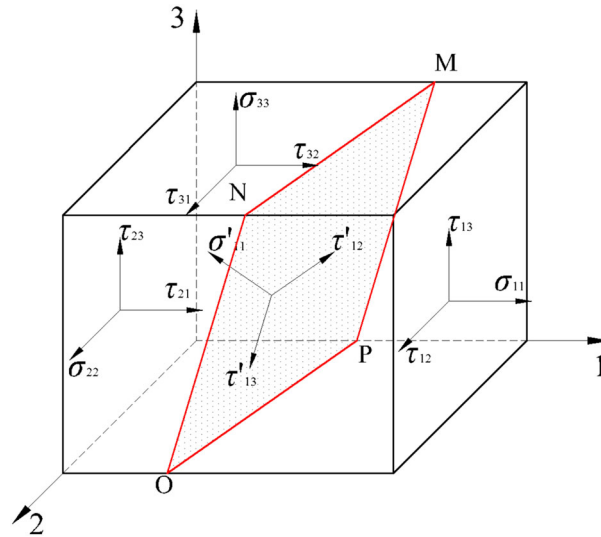


Fig. 2. Stress components on an arbitrary plane

The coordinate transformation matrix can be written as:

$$\mathbf{M} = \begin{bmatrix} \cos \theta - \sin \theta \cos \varphi & \sin \theta \sin \varphi \\ \sin \theta & \cos \theta \cos \varphi - \cos \theta \sin \varphi \\ 0 & \sin \varphi & \sin \varphi \end{bmatrix} \quad (6)$$

Through the coordinate transformation matrix, the stress tensor and strain tensor on an arbitrary material plane passing through the dangerous point in the new coordinate system can be obtained:  $\sigma'_{ij} = \mathbf{M}^T \sigma_{ij} \mathbf{M}$ ,  $\varepsilon'_{ij} = \mathbf{M}^T \varepsilon_{ij} \mathbf{M}$ .

## 2.2. Determination of the Critical Plane

The concept of critical plane is put forward based on the fatigue damage mechanism with certain physical significance, and the critical plane approach (CPA) is more effective for multiaxial fatigue life prediction [15]. The energy method generally takes energy as the damage parameter, which is a scalar that cannot illustrate the location and direction of crack initiation and propagation. However, the coordinate transformation matrix can give the physical interpretations of fatigue crack initiation and propagation in the energy method, and provide a theoretical basis for determining the location of the critical plane in the energy method. In this section, an energy-critical plane approach is proposed to determine the location of the critical plane.

Under multiaxial loading, the stress state of a typical element at the root of notch is shown in Fig. 2 [15].

The stress components on an arbitrary material plane MNOP are  $\sigma'_{11}$ ,  $\tau'_{12}$ , and  $\tau'_{13}$ , respectively, and the function of strain energy density with respect to  $\theta$  and  $\varphi$  is:

$$f(\theta, \varphi) = (1/2)(\sigma'_{11}\varepsilon'_{11} + \sigma'_{12}\varepsilon'_{12} + \sigma'_{13}\varepsilon'_{13}) \quad (7)$$

where  $\sigma'_{1i} = (\sigma_{11}\mathbf{M}_{11}^T + \sigma_{21}\mathbf{M}_{12}^T + \sigma_{31}\mathbf{M}_{13}^T)\mathbf{M}_{1i} + (\sigma_{12}\mathbf{M}_{11}^T + \sigma_{22}\mathbf{M}_{12}^T + \sigma_{32}\mathbf{M}_{13}^T)\mathbf{M}_{2i} + (\sigma_{13}\mathbf{M}_{11}^T + \sigma_{23}\mathbf{M}_{12}^T + \sigma_{33}\mathbf{M}_{13}^T)\mathbf{M}_{3i}$ ; and  $\varepsilon'_{1j} = (\varepsilon_{11}\mathbf{M}_{11}^T + \varepsilon_{21}\mathbf{M}_{12}^T + \varepsilon_{31}\mathbf{M}_{13}^T)\mathbf{M}_{1j} + (\varepsilon_{12}\mathbf{M}_{11}^T + \varepsilon_{22}\mathbf{M}_{12}^T + \varepsilon_{32}\mathbf{M}_{13}^T)\mathbf{M}_{2j} + (\varepsilon_{13}\mathbf{M}_{11}^T + \varepsilon_{23}\mathbf{M}_{12}^T + \varepsilon_{33}\mathbf{M}_{13}^T)\mathbf{M}_{3j}$ ; where  $i, j = 1, 2, 3$ , in order to simplify the calculation process, let  $(*)_d = (1/2)[(*)_{11} - (*)_{22}]$ , and  $(*)_m = (1/2)[(*)_{11} + (*)_{22}]$ , with the symbol '\*' denoting stress  $\sigma$  or strain  $\varepsilon$ .

Thus, the strain energy density function can be expressed as:

$$f(\theta, \varphi) = (1/2)[\sigma_m\varepsilon_m + \sigma_d\varepsilon_d + \sigma_{12}\varepsilon_{12} - \sigma_{33}\varepsilon_{33} - (\sigma_m\varepsilon_d + \sigma_d\varepsilon_m)\cos(2\theta) - (\sigma_m\varepsilon_{12} + \sigma_{12}\varepsilon_m)\sin(2\theta)]\sin^2\varphi + \sigma_{33}\varepsilon_{33} \quad (8)$$

By calculating the stationary points of Eq. (8), the values of  $\theta$  and  $\varphi$  at the extreme points can be obtained, and the location of the critical plane, on which fatigue cracks are easy to initiate, can be determined by  $\theta$  and  $\varphi$  further. The specific solution process is shown as follows.

Take the partial derivative of  $f(\theta, \varphi)$  with respect to  $\varphi$ :

$$\begin{aligned} \partial f(\theta, \varphi)/\partial \varphi = & [\sigma_m \varepsilon_m + \sigma_d \varepsilon_d + \sigma_{12} \varepsilon_{12} - \sigma_{33} \varepsilon_{33} - (\sigma_m \varepsilon_d + \sigma_d \varepsilon_m) \cos(2\theta) \\ & - (\sigma_m \varepsilon_{12} + \sigma_{12} \varepsilon_m) \sin(2\theta)] \sin \varphi \cos \varphi \end{aligned} \quad (9)$$

Let  $\partial f(\theta, \varphi)/\partial \varphi = 0$ , get  $\varphi = 90^\circ$  or  $\varphi = 0^\circ$ .

Take the partial derivative of  $f(\theta, \varphi)$  with respect to  $\theta$ :

$$\partial f(\theta, \varphi)/\partial \theta = 0 = [(\sigma_m \varepsilon_d + \sigma_d \varepsilon_m) \sin(2\theta) - (\sigma_m \varepsilon_{12} + \sigma_{12} \varepsilon_m) \cos(2\theta)] \sin^2 \varphi \quad (10)$$

Let  $\partial f(\theta, \varphi)/\partial \theta = 0$ , get:

- When  $\varphi = n\pi$ ,  $n = (0, 1, 2)$ ,  $\theta$  is an arbitrary value, which is not consistent with the actual situation, so it should be discarded.
- When  $\varphi \neq n\pi$ ,  $\tan(2\theta) = \frac{\sigma_m \varepsilon_{12} + \sigma_{12} \varepsilon_m}{\sigma_m \varepsilon_d + \sigma_d \varepsilon_m}$ , which is consistent with the actual situation, so the location of the critical plane can be expressed as follows:

$$\theta = \frac{1}{2} \arctan \left( \frac{\sigma_m \varepsilon_{12} + \sigma_{12} \varepsilon_m}{\sigma_m \varepsilon_d + \sigma_d \varepsilon_m} \right), \varphi = 90^\circ \quad (11)$$

With the help of FEM, the stress and strain components at the dangerous points can be extracted, and the position of the critical plane can be calculated by combining the coordinate transformation matrix and Eq. (11).

### 2.3. Determination of Critical Distance

The key to TCD is how to determine the critical distance  $L_0$ . Taylor [9] initially thought that the value of critical distance was related to material parameters. Soon afterward, Susmel and Taylor [13] found that the critical distance was a function related to fatigue life in the study of mid-cycle fatigue, and believed that the smaller was the number of cycles of fatigue crack initiation, the higher was the value of the critical distance. Naik [16] and Lanning [17] believed that the critical distance was related to the stress concentration factor of the notch. On the basis of Susmel and Taylor's model, Yang and Huang [18] introduced the stress concentration factor  $K_t$  to modify the relationship between life and critical distance. Recently, when Susmel and Taylor [19] were studying low-cycle fatigue, they believed that the critical distance was a material constant, which had nothing to do with the geometry of the notch, the external loading, or the number of failure cycles. Shen [20] also believed that the critical distance was a constant related to the material.

In engineering practice, different notch shapes and notch sizes will cause different stress gradient effects. Therefore, the geometrically similar notched specimens have different fatigue behaviors, which is called the geometric size effect [21]. Existing experiments show that the notch effect becomes more obvious with the decrease in the notch size when specimens have the same stress concentration factor and if the notch size is reduced to a certain value; and further reduction will not affect the fatigue strength of specimens [22]. Therefore, if the traditional notch effect method is directly applied to the study of geometric size effect, there will be some obstacles. In 1961, Kuguel [23] originally proposed the highly stressed volume (HSV) method in consideration of the geometric size effect, a lower limit of high stress volume  $\sigma_{HSV}$  was defined and the material element volume between the maximum stress and the lower limit of high stress was regarded as the high stress volume.

$$\sigma_{HSV} = m\% \sigma_{c, \max} \quad (12)$$

where  $\sigma_{c, \max}$  represents the maximum stress in the local region of the notch, and  $m\%$  is an empirical parameter used to define the scale of high stress volume.

According to the HSV theory, the probability of crack initiation and propagation increases with the increase in high stress volume, which leads to eventual fatigue failure [24]. Hence, in fatigue analysis, it is not necessary to analyze the stress state for the whole specimen, but close attention needs to be paid to the critical region with higher stress to obtain more reliable prediction results. According

to experience, Kuguel proposed that the empirical parameter  $m$  should be 95, that is, 95% of high stress volume standard (V95 standard). Subsequently, many scholars conducted relevant studies and verified its reliability based on this standard [25]. However, the HSV method needs the calculation of the number and volume of high stress elements, which leads to a lot of work.

In this paper, the high stress volume is simplified as a specified high stress line segment (SHSL) on the critical plane based on the HSV method and Kuguel's theory. The maximum equivalent stress of dangerous point is recorded, and the value corresponding to 95% of the maximum equivalent stress is calculated as  $\sigma_{\text{SHSL}}$ ,

$$\sigma_{\text{SHSL}} = 95\% \sigma_{\text{eqv,max}} \quad (13)$$

where  $\sigma_{\text{eqv,max}}$  is the maximum equivalent stress.

Based on Eq. (13), the equivalent stress along the SHSL on the critical plane is extracted and the distance between the dangerous point and the critical point of 95% of the maximum equivalent stress is defined as the critical distance.

### 3. Determination of Impact Factor of Equivalent Stress Gradient

In the elastic-plastic deformation stage and the fracture process, fatigue properties of metal materials are inevitably affected by the notch effect [1], which produces local stress concentration at the notch root. Under external loading, stress in the vicinity of the notch gradually decreases from the surface of the specimen to the interior of the material, forming a certain stress gradient. The stress gradients of specimens with different notch sizes and shapes at the notch are not the same for specimens with the same nominal stress. Research shows that when the notch is accompanied by a large stress gradient, the fatigue strength of the notched specimen changes significantly [7]. Taking the influence of stress gradient into account can significantly improve the fatigue life prediction accuracy of notched specimens. Wang [26] studied the influence of stress gradient on fatigue life under uniaxial loading and defined the uniaxial stress gradient impact factor  $Y_a$  through the idea of stress normalization. Its expression is shown as:

$$Y_a = \frac{1}{2S_{0.5}} \quad (14)$$

where  $S_{0.5}$  is the area bounded by the normal stress normalization curve and the abscissa in the interval of  $0 \leq x/r \leq 0.5$ , with  $x/r$  the abscissa of the curve, and  $x$  the distance from the notch root.

When there is no notch in the specimen, the internal stress is evenly distributed, and the stress gradient impact factor is 1, so the fatigue strength of the specimen is not affected by the stress gradient. When there is a notch in the specimen, the stress gradient impact factor is  $< 1$ . The area parameter of stress normalization curve is used to define the influence of stress gradient, which can avoid the numerical error caused by the derivative when calculating the stress gradient.

In this paper, the above idea is introduced to the fatigue damage assessment of multiaxial notched specimens. The curvature radius  $r$  is selected as the normalized cardinality of distance  $x$  in this method, but this selection is sometimes limited by the notch shape. For instance, for the deep U-notched and semicircular-notched specimens with the same radius of curvature, although the radii of curvature of notches are the same, the degrees of weakening of the shaft by the notch are different, which results in different stress distributions and stress gradients around the notch. Therefore, in this paper, the normal stress is replaced by the von Mises equivalent stress, the radius of curvature  $r$  is modified as the critical distance  $L_0$  on the critical plane, and the multiaxial equivalent stress gradient impact factor  $Y_m$  is obtained as:

$$Y_m = \frac{1}{2S_{\text{eqv},0.5}} \quad (15)$$

where  $S_{\text{eqv},0.5}$  is the area bounded by the von Mises equivalent stress normalization curve and the abscissa in the interval of  $0 \leq x/L_0 \leq 0.5$ , with  $x/L_0$  the abscissa of the curve.

### 4. Multiaxial Proportional Fatigue Experiments

In this paper, Q345 steel was selected as the test material. The mechanical properties and uniaxial fatigue property parameters are listed as follows [15]: elastic modulus  $E = 1.92 \times 10^5$  MPa, yield

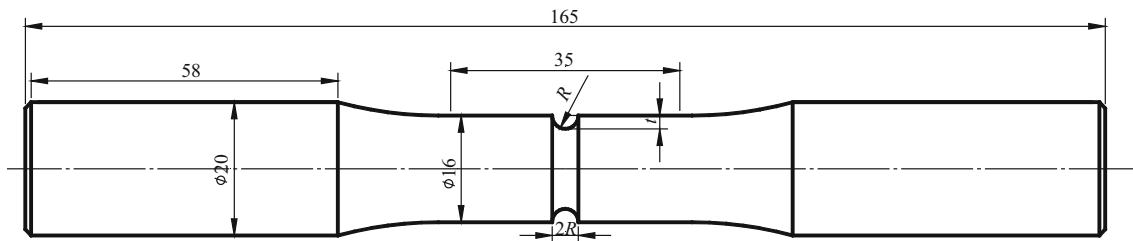


Fig. 3. Notched specimen-A bar (mm)

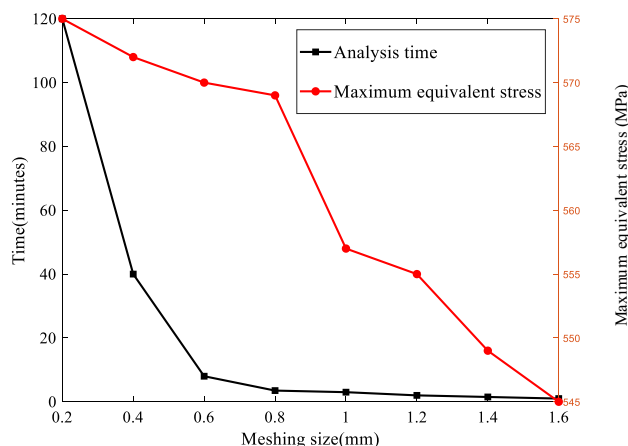


Fig. 4. The relationship between mesh size and calculation accuracy/analysis time

stress  $\sigma_y = 476$  MPa, ultimate stress  $\sigma_u = 625$  MPa, Poisson’s ratio  $\nu = 0.3$ , cyclic strength coefficient  $K = 2.85 \times 10^3$  MPa, fatigue strength coefficient  $\sigma'_f = 1.44 \times 10^3$  MPa, cyclic strain hardening exponent  $n = 0.378$ , fatigue strength exponent  $b = -0.159$ , fatigue ductility coefficient  $\epsilon'_f = 0.249$ , and fatigue ductility exponent  $c = -0.494$ . The geometries and dimensions of grooved shaft specimens are presented in Fig. 3. The fatigue experiment was carried out on Instron 8850 tension–torsion fatigue test machine, and the axial strain and tangential strain were controlled by Epsilon3550 tension–torsion extensor. The phase difference between the axial strain and the tangential strain during the test process was  $0^\circ$  (proportional loading); the loading frequencies of tension–compression and torsion were both 1 Hz. In this paper, the fracture of the specimens was defined as the failure criterion, and tests were carried out three times for each working condition to get the average value  $N_t$ .

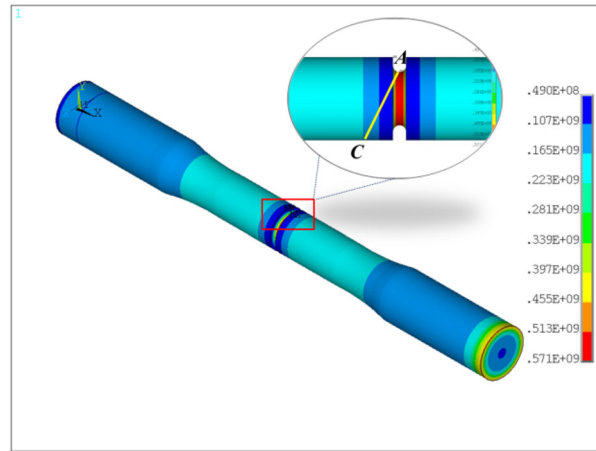
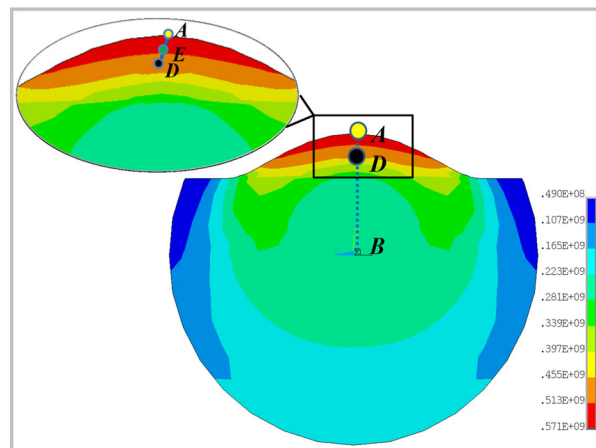
### 5. Finite Element Analysis of Notched Specimens

Nowadays, the FEM has become a prime method for fatigue strength analysis and life prediction [22]. In this paper, the distribution of elasto-plastic stress/strain in the vicinity of the notch root is extracted by using the FE software with 8-node element Solid 185. The MKIN model which includes the Bauschinger effect is used to define the stress–strain relationship of the materials [Eq. (16)]. During the modeling, the specimens are reasonably cut to successfully generate a mapped mesh. During the whole process of FE calculation, both the calculation accuracy and the calculation efficiency should be taken into account. Figure 4 shows the relationship between the mesh size and analysis time/calculation accuracy.

$$\epsilon = \begin{cases} \frac{\sigma}{E} & (\epsilon \leq \epsilon_y) \\ \frac{\sigma_y}{E} + \left(\frac{\sigma}{K}\right)^{\frac{1}{n}} & (\epsilon > \epsilon_y) \end{cases} \quad (16)$$

It can be seen from Fig. 4 that the maximum equivalent stress of notch root decreases with the increase in mesh size. When the mesh size is  $< 0.8$  mm, the equivalent stress keeps steady, while the equivalent stress has a big deviation when the mesh size is  $> 0.8$  mm. Meanwhile, the analysis time



Fig. 5. Notched specimen equivalent stress nephogram of  $NL_1$ Fig. 6. Equivalent stress nephogram on the critical plane of  $NL_1$ 

reduces tardily with the increase of mesh size. However, when the mesh size is  $< 0.6$  mm, the analysis time increases rapidly. Finally, both calculation accuracy and efficiency are taken into consideration, the mesh size in the vicinity of notch root is set as 0.8 mm, and the mesh size for the remainder of the specimen is set as 4 mm. When loading, one end of the specimen is fixed, another end is subjected to proportional tension–torsion. The torsion is converted into torsion angle, and the axial load is converted into axial displacement, which are uniformly applied onto all nodes of the outermost circle of the loading end.

The stress–strain history of notch root in a single cyclic load can be obtained. The position of the dangerous point, namely the maximum equivalent stress point, and the stress–strain components of the dangerous point under the basic coordinate system  $xyz$  can be extracted. Meanwhile, the position and direction of the critical plane is determined according to the steps of Sect. 1.

The equivalent stress nephogram under each working condition can be acquired. Taking  $NL_1$  (Fig. 5) as an example for a specific explanation, the working plane is rotated by  $(90^\circ, 90^\circ, \theta)$  to make it coincide with the critical plane (AC plane), then the specimen is cut by the working plane, and the equivalent stress nephogram on the critical plane is further obtained (Fig. 6).

As can be seen from Fig. 6, the line segment AB is the specified path on the critical plane, and the equivalent stress along line AB is firstly extracted. Then, the length corresponding to  $\sigma_{SHSL}$  (here,  $\sigma_{SHSL} = 95\% \sigma_{eqv,max}$ , with  $\sigma_{eqv,max}$  the equivalent stress at point A) on AB is defined as the critical distance  $L_0$ . In this case,  $L_0$  is the length of line segment AD.



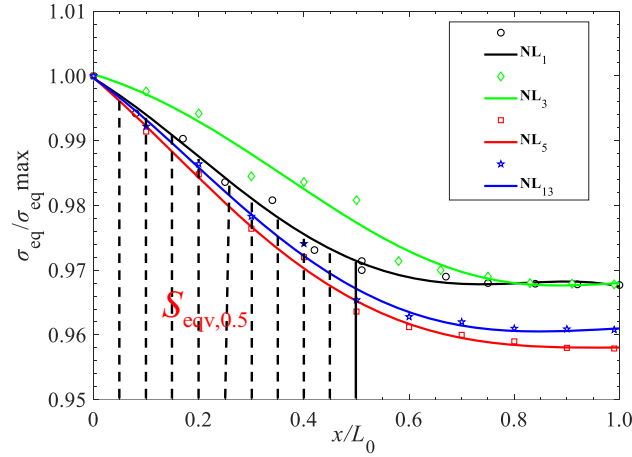


Fig. 7. Equivalent stress normalization–distance normalization curve

The local stress–strain approach (LSSA) takes the maximum stress–strain value at the dangerous point as the fatigue damage parameter to predict the fatigue life of notched specimens. In this paper, combining the PM of TCD [Eq. (1)] and the LSSA, considering the combined effect of the equivalent stress  $\sigma_{eqv,max}$  at point A and the equivalent stress  $\sigma_{eqv,E}$  at the midpoint of AD, which can be obtained according to the equivalent stress extracted by FEM on the AB path, a new effective stress is defined as:

$$\sigma_{eff} = \sqrt{\sigma_{eqv,max}\sigma_{eqv,E}}, \quad L_{AE} = \frac{1}{2}L_{AD} = \frac{1}{2}L_0 \quad (17)$$

where  $L_{AE}$  is the length of line AE.

With the help of Osgood Ramberg equation, the relationship between effective stress  $\sigma_{eff}$  and strain  $\varepsilon_{eff}$  on critical plane under multiaxial proportional loading is given, and the effective strain  $\varepsilon_{eff}$  is obtained as

$$\frac{\varepsilon_{eff}}{2} = \frac{\sigma_{eff}}{2E} + \left(\frac{\sigma_{eff}}{2K}\right)^{\frac{1}{n}} \quad (18)$$

where  $n$  denotes the cyclic strain hardening index,  $K$  is the cyclic strength coefficient, and  $E$  represents Young's modulus.

In the 1950s, Manson and Coffin studied the low-cycle fatigue behaviors of more than 20 materials, and proposed the life prediction model suitable for low-cycle fatigue as follows.

$$\varepsilon_a = \frac{\sigma'_f}{E} (2N_f)^b + \varepsilon'_f (2N_f)^c \quad (19)$$

where  $\varepsilon_a$  is the strain amplitude.

The multiaxial equivalent stress gradient impact factor  $Y_m$  obtained by Eq. (15) is introduced to modify the Manson–Coffin equation. Taking  $NL_1$  as an example to explain the process of solving  $Y_{m-NL1}$ , the fifth-order polynomials are used to fit the equivalent stress normalization–distance normalization curve (Fig. 7), and obtain the equation  $\sigma_{eq}/\sigma_{eq,max} = I = 0.99951h^5 - 0.04607h^4 - 0.03269h^3 + 0.03521h^2 - 0.01407h + 0.00183$  ( $h = x/L_0$ ) and  $Y_{m-NL1} = 1/(2S_{eqv,0.5}) = 1/(2 \int_0^{0.5} I dh) = 1.0140$ . Meanwhile, the fatigue life prediction model for multiaxial notched specimens is established by substituting  $\varepsilon_{eff}$  for  $\varepsilon_a$ , then the prediction life using the proposed model ( $N_{pr}$ ) of the notched specimens can be calculated. Simultaneously, the prediction life using the LSSA ( $N_{pl}$ ) and the PM ( $N_{pp}$ ) can be calculated respectively, and the results are listed in Table 1.

$$\varepsilon_{eff} = Y_m \cdot \left\{ \frac{\sigma'_f}{E} (2N_f)^b + \varepsilon'_f (2N_f)^c \right\} \quad (20)$$

Table 1. Fatigue test results and prediction results

Load mode	$R/\text{mm}$	$t/\text{mm}$	$\varepsilon/\%$	$\gamma/\%$	$L_0/\text{mm}$	$Y_m$	$\sigma_{\text{eff}}/\text{MPa}$	$N_t/\text{cycles}$	$N_{\text{pr}}/\text{cycles}$	$N_{\text{pl}}/\text{cycles}$	$N_{\text{pp}}/\text{cycles}$
NL <sub>1</sub>	1.6	3.6	0.395	0.479	0.64	1.0140	560.69	12067	8895	8385	10411
NL <sub>2</sub>	1.6	3.2	0.395	0.479	0.53	1.0168	554.33	12865	9547	8905	5234
NL <sub>3</sub>	1.6	2.4	0.395	0.479	0.59	1.0214	555.08	13680	9634	9514	6455
NL <sub>4</sub>	1.6	1.6	0.395	0.479	0.58	1.0139	535.08	14936	11637	9951	5779
NL <sub>5</sub>	1.28	4.0	0.395	0.479	0.59	1.0204	606.21	8963	5797	5642	2441
NL <sub>6</sub>	1.92	2.08	0.395	0.479	0.50	1.0370	546.73	15630	10954	9847	6595
NL <sub>7</sub>	1.28	3.6	0.347	0.408	0.49	1.0195	553.87	12934	9701	8760	5354
NL <sub>8</sub>	1.28	3.6	0.347	0.347	0.50	1.0197	554.38	13391	9627	9347	4095
NL <sub>9</sub>	1.28	3.6	0.347	0.295	0.50	1.0347	560.10	15563	9488	10501	3462
NL <sub>10</sub>	1.92	3.6	0.347	0.408	0.51	1.0148	574.84	12152	7734	8342	4449
NL <sub>11</sub>	1.92	3.6	0.347	0.245	0.49	1.0160	545.08	13861	10537	8859	3967
NL <sub>12</sub>	1.92	3.6	0.347	0.200	0.76	1.0180	534.53	12962	11830	9714	3760
NL <sub>13</sub>	2.24	3.6	0.347	0.408	0.63	1.0163	567.21	12030	8386	8796	4759
NL <sub>14</sub>	2.24	3.6	0.295	0.408	0.75	1.0217	539.81	14165	11296	9544	8875
NL <sub>15</sub>	2.24	3.6	0.251	0.408	0.50	1.0165	540.64	13394	11020	9465	4331

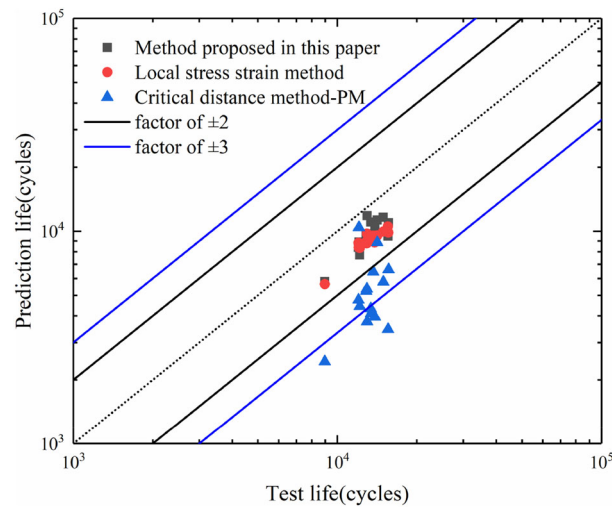


Fig. 8. The relation between predicted life and test life

It can be seen from Fig. 7 that the equivalent stress gradient changes with the notch size. When specimens have the same notch radius (NL<sub>1</sub> vs. NL<sub>3</sub>), the larger is the notch depth, the greater is the equivalent stress gradient; when specimens have the same notch depth (NL<sub>1</sub> vs. NL<sub>13</sub>), the larger is the notch radius, the greater is the equivalent stress gradient.

## 6. Results and Discussion

As can be seen from Table 1, the effective stress  $\sigma_{\text{eff}}$  is less than the peak stress  $\sigma_{\text{eqv,max}}$ . The test results  $N_t$  are compared with the prediction results, and the comparison results are depicted in Fig. 8.

It can be seen from Fig. 8 that, for the proposed method and the LSSA, all of the predicted points fall within the  $\pm 2$  scatter bands; while for the PM, most of the predicted points fall out of the  $\pm 2$  scatter bands, and there are several points falling out of the  $\pm 3$  scatter bands.

## 7. Conclusions

Based on TCD and the LSSM, considering the equivalent stress gradient at the notch and influence of size effect, a method for predicting the multiaxial fatigue life of notched specimens was given. This method was used to predict the fatigue life of U-notched Q345 steel specimens, and the prediction results were compared with the LSSA and the PM of TCD. The following conclusions can be obtained:

- (1) Based on the high stress volume method and Kuguel's Theory, the high stress volume is simplified as a high equivalent stress line segment on the critical plane. The equivalent stress along the specified path on the critical plane is extracted, and the peak stress is obtained. The distance between the dangerous point and the critical point (95% of the maximum equivalent stress) is defined as the critical distance  $L_0$ . Consequently, a simple method for determining the critical distance is given.
- (2) Based on Wang's idea of stress-distance normalization, the normal stress is replaced by the von Mises equivalent stress, the radius of curvature  $r$  is modified as the critical distance  $L_0$  on the critical plane, and a new multiaxial equivalent stress gradient impact factor  $Y_m$  is defined.
- (3) In this paper, the new method, the LSSA and the PM of TCD are used to predict the life of U-notched Q345 steel bars. Among the three methods, the error of the PM is larger, while the errors of the new method and LSSA are both within a factor of two error bands. Meanwhile, the prediction results of the new method are closer to the experimental life. This is because the traditional PM only considers the maximum principal stress at the specified point in the elastic stress field, while the new method takes the von Mises equivalent stress into consideration, which comprehensively considers effects of the three principal stresses  $\sigma_1$ ,  $\sigma_2$ , and  $\sigma_3$ . At the same time, on the basis of considering the effect of equivalent stress gradient, the equivalent stress at the dangerous point and the equivalent stress at the critical distance  $L_0/2$  are overall considered in the new method. The effective stress value  $\sigma_{\text{eff}}$  of the new method is less than the peak stress  $\sigma_{\text{eqv,max}}$ , which reduces the effect of peak stress and makes the result more accurate.

**Acknowledgements.** This research was supported by the National Natural Science Foundation of China (Grant No. 51605212), the Natural Science Foundation of Gansu Province (Grant No. 20JR10RA161), and the Project of Hongliu Excellent Youth Program of Lanzhou University of Technology (Grant No. 2020062001).

## References

- [1] Branco R, Prates PA, Costa JD. Rapid assessment of multiaxial fatigue lifetime in notched components using an averaged strain energy density approach. *Int J Fatigue*. 2019;124:89–98.
- [2] Liao D, Zhu SP. Energy field intensity approach for notch fatigue analysis. *Int J Fatigue*. 2019;127:190–202.
- [3] Tanaka K, Akiniwa Y. Fatigue crack propagation behavior derived from S–N data in very high cycle regime. *Fatigue Fract Eng Mater Struct*. 2002;25(8–9):775–84.
- [4] Luo P, Yao WX, Wang YY, Li P. A survey on fatigue life analysis approaches for metallic notched components under multi-axial loading. *J Aerosp Eng*. 2019;233:3870–90.
- [5] Zeng Y, Li MQ, Zhou Y, Li N. Development of a new method for estimating the fatigue life of notched specimens based on stress field intensity. *Theor Appl Fract Mech*. 2019;104:1–14.
- [6] Matteo B, Ciro S. Mean stress and plasticity effect prediction on notch fatigue and crack growth threshold, combining the theory of critical distances and multiaxial fatigue criteria. *Fatigue Fract Eng Mater Struct*. 2019;42(6):228–1246.
- [7] Liao D, Zhu SP, Qian GI. Multiaxial fatigue analysis of notched components using combined critical plane and critical distance approach. *Int J Mech Sci*. 2019;2019(160):38–50.
- [8] Taylor D, Bologna P, Knani KB. Prediction of fatigue failure location on a component using a critical distance method. *Int J Fatigue*. 2000;22(9):735–42.
- [9] Neuber H. Theory of notch stresses: principles for exact stress calculation. Ann Arbor: Edwards Brothers, Inc; 1946.
- [10] Re P. Notch sensitivity. *Metal fatigue*. New York: McGraw-Hill; 1959.
- [11] Taylor D. Geometrical effects in fatigue: a unifying theoretical model. *Int J Fatigue*. 1999;21(5):413–20.
- [12] Bellett D, Taylor D, Marco S. The fatigue behaviour of three-dimensional stress concentrations. *Int J Fatigue*. 2005;27(3):207–21.
- [13] Susmel L, Taylor D. A critical distance/plane method to estimate finite life of notched components under variable amplitude uniaxial/multiaxial fatigue loading. *Int J Fatigue*. 2011;38:7–24.
- [14] Wu ZR, Hu XT, Song YD. Estimation method for fatigue life of notched specimen under multi-axial loading. *J Eng Mech*. 2014;31(10):216–21 ((in chinese)).
- [15] Liu JH, Ran Y, Xie LJ, Xue WZ. Multiaxial fatigue life prediction method of notched specimens considering stress gradient effect. *Fatigue Fract Eng Mater Struct*. 2021;44:1406–19.
- [16] Naik RA, Lanning DB, Nicholas T. A critical plane gradient approach for the prediction of notched HCF life. *Int J Fatigue*. 2004;27(5):481–92.
- [17] Lanning DB, Nicholas T, Haritos GK. On the use of critical distance theories for the prediction of the high cycle fatigue limit stress in notched Ti-6Al-4V. *Int J Fatigue*. 2004;27(1):45–57.

- [18] Huang J, Yang XG, Shi DQ. Low cycle fatigue life prediction of notched DZ125 component based on combined critical distance-critical plane approach. *J Mech Eng.* 2013;49(22):109–15 ((in chinese)).
- [19] Susmel L, Taylor D. An elasto-plastic reformulation of the theory of critical distances to estimate lifetime of notched components failing in the low/medium-cycle fatigue regime. *J Eng Mater Technol.* 2010;132(2):21–8.
- [20] Shen JB, Tang DL. Predicting method for fatigue life with stress gradient. *Chin J Mech Eng.* 2017;28(01):40–4 ((in chinese)).
- [21] Zhu SP, Ai Y, Liao D, Correia JAFO. Recent advances on size effect in metal fatigue under defects: a review. *Int J Fract.* 2021. <https://doi.org/10.1007/s10704-021-00526-x>.
- [22] Lukas P, Kunz L. Notch size effect in fatigue. *Fatigue Fract Eng Mater Struct.* 1989;12(3):175–86.
- [23] Kuguel R. A relation between theoretical stress concentration factor and fatigue notch factor deduced from the concept of highly stressed volume. *Proc ASTM.* 1961;61:732–48.
- [24] Torrent RJ. A general relation between tensile strength and specimen geometry for concrete-like materials. *Mater Constr.* 1977;10(4):187–96.
- [25] Lin CK, Lee WJ. Effects of highly stressed volume on fatigue strength of austempered ductile irons. *Int J Fatigue.* 1998;20(4):301–7.
- [26] Wang YR, Li HX, Yuan SH. Method for notched fatigue life prediction with stress gradient. *J Aero Power.* 2013;28(06):1208–14.